The magnetic structure of $Fe_{0.91}Zr_{0.09}$ metallic glass

1999 J. Phys.: Condens. Matter 11 9249

(http://iopscience.iop.org/0953-8984/11/47/310)

J. Phys.: Condens. Matter **11** (1999) 9249–9262. Printed in the UK PII: S0953-8984(99)06788-0

The magnetic structure of $Fe_{0.91}Zr_{0.09}$ metallic glass

L Karlsson†, R L McGreevy† and J D Wicks‡§

† Studsvik Neutron Research Laboratory, Uppsala University, S-611 82 Nyköping, Sweden
‡ Department of Physics, Clarendon Laboratory, Oxford University, Parks Road, Oxford OX1 3PU, UK

Received 9 August 1999

Abstract. Models of the atomic and magnetic structures of $Fe_{0.91}Zr_{0.09}$ metallic glass have been produced by RMC modelling of neutron diffraction and x-ray diffraction data at temperatures between 10 and 300 K. The magnetic structure at all T is predominantly ferromagnetic but a weak peak in the neutron structure factor at 1.2 $Å^{-1}$ is identified as being due to magnetic 'defects'. It is found that the average local density of Fe atoms around these defects tends to be higher than around 'normal' moments. This supports the idea of magnetic frustration in such systems due to competing ferromagnetic and antiferromagnetic interactions. Assuming that Fe and Zr substitute isomorphously in $Fe_{1-x}Zr_x$ glasses, and that Fe moments with more than 12 neighbouring Fe atoms behave antiferromagnetically, the composition dependence of the magnetic phase diagram can be explained on the basis of the RMC structural model for $Fe_{0.91}Zr_{0.09}$ glass.

1. Introduction

One of the main problems in diffraction studies of the magnetic structure of magnetic glasses is the need to separate the magnetic and nuclear contributions to the scattering. This can be done using polarized neutrons, but it is difficult and only possible at one or two places in the world. In a very few cases isotopic substitution can be used. However, even if the contributions have been separated, it is still necessary to know the three dimensional atomic structure before the effects of the local structure can be separated from those of magnetic interactions. A possible solution to both these problems is the use of the reverse Monte Carlo (RMC) modelling technique, where atomic and magnetic structures are modelled simultaneously. With the RMC modelling method it is possible to incorporate data from many different experimental methods such as neutron diffraction, x-ray diffraction and EXAFS.

The RMC method has been previously applied to studies of $Dy_{0.7}Ni_{0.3}$ based glasses [1–3] and $Dy_{0.7}Fe_{0.3}$ [4]. These are optimized systems because the atomic structure has been determined from isotopic substitution of both Dy and Ni [5], and $Dy_{0.7}Fe_{0.3}$ is structurally isomorphous with $Dy_{0.7}Ni_{0.3}$. In this paper we report the results of the first study where atomic and magnetic structures have been modelled simultaneously. The $Fe_{0.91}Zr_{0.09}$ glass has been chosen for two reasons. Firstly the magnetic behaviour changes considerably with small composition changes in this region, so the magnetic effects have to be understood in the framework of an almost invariant atomic structure. Secondly many different structural measurement techniques can be used on this sample. The absorption edges of both Fe and Zr occur at suitable energies so that anomalous x-ray scattering could be used, and these energies are sufficiently separated that the EXAFS spectra do not overlap. The modelling is in fact based

§ Current address: 64 Saltmarsh, Orton Malborne, Peterborough, Cambs. PE2 5NL, UK.

0953-8984/99/479249+14$30.00

on data from neutron diffraction (using both pulsed source and reactor-based techniques) and x-ray diffraction. In addition we have performed a differential anomalous x-ray scattering measurement at the Zr edge. The anomalous scattering shows that the local Zr environment is not significantly different from that of Fe (i.e. the total x-ray diffraction pattern is the same as the differential pattern) but the statistical accuracy is poor and so these data have not been used for modelling.

A number of models of the magnetic structure of $Fe_{1-x}Zr_x$ glasses already exist, though these are based on techniques such as magnetization/susceptibility measurements and Mössbauer spectroscopy rather than diffraction. They can basically be divided into three categories:

(a) Ferromagnetic order in the z-direction with spin glass freezing in the x–y-directions (e.g. [6]).
(b) A ferromagnetic Fe matrix containing antiferromagnetic Fe clusters (e.g. [7]).
(c) A ferromagnetic Fe matrix containing ferromagnetic Fe clusters (e.g. [8]).

The magnetic ordering temperatures, T_c, measured by different authors, tend to be consistent within a few degrees (e.g. $T_c = 218$ K for $Fe_{0.91}Zr_{0.09}$ [9]), suggesting that differences in models are not due to differences in samples. However one general problem is that these models are not specific about the length scales over which they are supposed to apply (e.g. how large is a cluster?), so this produces some difficulty in discussing them in relation to the models produced here, which are specifically relevant to the short range magnetic order on a length scale of $\leqslant 20$ Å.

2. Experimental details

A sample of the amorphous alloy $Fe_{0.91}Zr_{0.09}$ was prepared by melt spinning. The ribbons were approximately 1 mm wide and 22 μm thick. X-ray measurements were made at Daresbury Laboratory (UK) using the Synchrotron Radiation Source (SRS). Diffraction studies were done on Station 9.1, the high precision powder diffractometer, set up in Warren–Mavel mode at the Ag K edge to suppress Compton scattering. A single strip, without pin-hole defects, was mounted on an aluminium ring with an inner diameter of 25 mm. As the sample width was 1 mm, a beam size of 0.5 mm $\times$ 10 mm and symmetrical transmission geometry was used. The experiment was carried out at room temperature and the data were corrected using the free atom form factor for Fe^{2+}.

For neutron diffraction the sample was packed tightly and sealed inside a standard vanadium container. A time-of-flight neutron diffraction experiment was carried out using the Liquids and Amorphous Materials Diffractometer (LAD) at the neutron spallation source, ISIS, at the Rutherford–Appleton Laboratory (UK). The sample was placed inside a cryostat and measured at 10, 100, 200 and 300 K. The data extend from $Q = 0.3$ to 49.2 Å^{-1}; for $Q > 20$ Å^{-1} the structure factor is essentially flat, which shows that the sample is completely amorphous. In order to confirm the existence of a weak peak at low Q (see below), which happened to occur at a 'join' between data from two LAD detector banks, a second neutron diffraction experiment was carried out on the same sample using the Studsvik Liquids and Amorphous Materials Diffractometer (SLAD) at the R2 reactor, Studsvik Neutron Research Laboratory (Sweden). Data were collected at 10, 150, 200, 250 and 300 K. The data from LAD and SLAD are in good agreement. Corrected total structure factors are shown in figure 1. The structure factor for $Q > 0.7$ Å^{-1} is essentially invariant in this temperature range; there is only a small change at the main peak. The weak peak at 1.2 Å^{-1} was reproduced in both LAD and SLAD data, but there was no evidence of such a feature in the x-ray data. This feature must

therefore be magnetic in origin. More recent measurements [10] above ambient temperature indicate that the low Q scattering decreases rapidly, but the 1.2 $Å^{-1}$ peak is almost unchanged until the sample crystallizes at about 600 K.

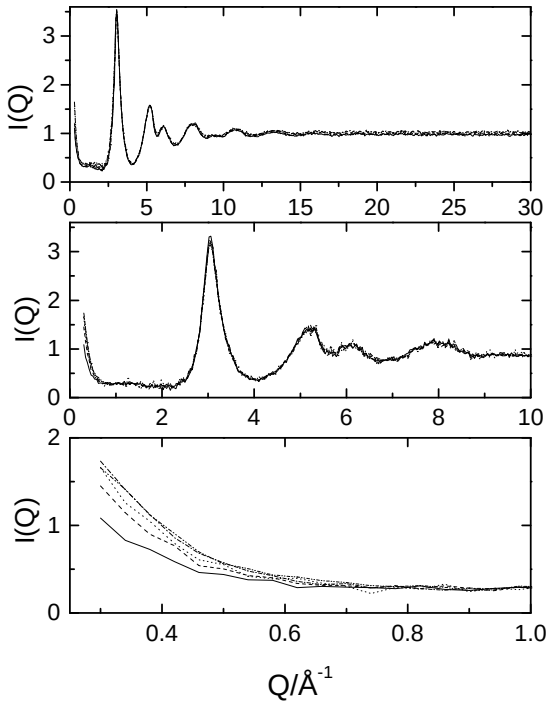

Figure 1. Total structure factors for $Fe_{0.91}Zr_{0.09}$ measured by neutron diffraction. Top: LAD data at 10 (solid curve), 100 (dash), 200 (dot) and 300 K (dash–dot). Centre: SLAD data at 10 (solid curve), 150 (dash), 200 (dot), 250 (dash–dot) and 300 K (dash–dot–dot). Bottom: the low Q region on an expanded scale.

3. Theoretical formalism

For coherent x-ray scattering the total structure factor is given by

$$F_x(Q) = \sum_{\alpha=1}^{n}\sum_{\beta=1}^{n} c_\alpha c_\beta f_\alpha(Q) f_\beta(Q)[A_{\alpha\beta}(Q) - 1] \tag{1}$$

where $A_{\alpha\beta}(Q)$ are the partial structure factors, n is the number of species, c_α is the concentration of species α and $f_\alpha(Q)$ is the atomic form factor for species α. In the non-relativistic approximation the atomic form factor is

$$f_\alpha(Q) = \int \psi_f^*(r)\, \mathrm{e}^{\mathrm{i}Qr}\, \psi_i(r)\, \mathrm{d}^3 r. \tag{2}$$

ψ is the total wave function of the atom and the subscripts i and f refer to the initial and final states respectively. For coherent scattering these states are the same.

Using the assumption that the nuclear and magnetic contributions to the scattering of neutrons are additive for a disordered magnetic system with one magnetic component, the

total (coherent) structure factor $I(Q)$ is given by

$$I(Q) = F(Q) + \sum_{\alpha=1}^{n} c_\alpha b_\alpha^2 + I_M(Q) \tag{3}$$

where b_α is the coherent scattering length for atomic species α, and

$$F(Q) = \sum_{\alpha=1}^{n}\sum_{\beta=1}^{n} c_\alpha c_\beta b_\alpha b_\beta [A_{\alpha\beta}(Q) - 1]. \tag{4}$$

The magnetic structure factor is defined using the formalism of Blech and Averbach [11],

$$I_M(Q) = \left(\frac{\mathrm{d}\sigma}{\mathrm{d}\Omega}\right)_p + \left(\frac{e^2\gamma}{2m_e c^2}\right)^2 c_M f_M^2(Q) \times \int \left[A(r)\frac{\sin(Qr)}{Qr} + B(r)\left(\frac{\sin(Qr)}{(Qr)^3} - \frac{\cos(Qr)}{(Qr)^2}\right)\right] \mathrm{d}r \tag{5}$$

where the paramagnetic scattering is

$$\left(\frac{\mathrm{d}\sigma}{\mathrm{d}\Omega}\right)_P = \frac{2}{3}c_M + \left[\frac{e^2\gamma}{2m_e c^2}\mu f_M(Q)\right]^2. \tag{6}$$

c_M is the concentration of the magnetic species, $(e^2\gamma/m_e c^2)^2 = 0.29 \times 10^{-24}$ cm^2, μ is the magnitude of the magnetic moment (in μ_B) and $f_M(Q)$ is the magnetic form factor for neutrons [12].

$$A(r) = 4\pi r^2 g_{MM}(r)\langle \mu_\perp(\mathbf{0}) \cdot \mu_\perp(\boldsymbol{r})\rangle \tag{7}$$

and

$$B(r) = 4\pi r^2 g_{MM}(r)[2\langle \mu_\parallel(\mathbf{0}) \cdot \mu_\parallel(\boldsymbol{r})\rangle - \langle \mu_\perp(\mathbf{0}) \cdot \mu_\perp(\boldsymbol{r})\rangle] \tag{8}$$

where $g_{MM}(r)$ is the partial radial distribution function for the magnetic atom. $\langle \mu_\parallel \cdot \mu_\parallel\rangle_r$ and $\langle \mu_\perp \cdot \mu_\perp\rangle_r$ are the correlations of the components of the moment parallel and perpendicular to the vector joining two moments at $\mathbf{0}$ and $\boldsymbol{r}$, known as the radial and tangential correlations respectively.

In the RMC model the moment–moment correlation function $\langle \mu \cdot \mu\rangle_r$ at distance r is defined as

$$\langle \mu \cdot \mu\rangle_r = \frac{n_\mu(r)}{4\pi r^2 \mathrm{d}r\ \rho c_M} - \sum_{0}^{R} n_\mu(r)/\tfrac{4}{3}\pi R^3 \rho c_M \tag{9}$$

where $n_\mu(r)$ is the sum of $\mu(\mathbf{0}) \cdot \mu(\boldsymbol{r})$ for atoms at a distance between r and $r + \mathrm{d}r$ from a central magnetic atom, averaged over all magnetic atoms as centres. R is half the length of the (cubic) configuration box and ρ is the number density of ions. The spin-spin correlation function $\langle \mu \cdot \mu\rangle_r$ has a similar form to the familiar atomic radial distribution function $g(r)$, but unlike the atomic case it is not in general possible to obtain it by direct Fourier transform of the magnetic structure factor. Except for the limiting cases of complete spin disorder (paramagnetism) when the second term of $I_M(Q)$ is zero, or complete ferromagnetic order, when $B(r)$ goes to zero, computer modelling is required to determine the magnetic structure.

4. RMC modelling

In this study we have used x-ray data to provide information on the atomic structure, while the neutron data provide information on both atomic and magnetic structures. Initially difficulties

were experienced with obtaining consistency between all of the data sets within a single structural model. Some problems were overcome by development of the program RMCSPIN to enable simultaneous modelling of both atomic and magnetic structures, which indicated a need to renormalize the x-ray diffraction data. It was found that a moment of 2.2 μ_B was most consistent with the neutron data; this is the same value as predicted theoretically [13, 15]. Lorenz and Hafner [14] have also (theoretically) identified a small moment on the Zr atom. However this moment is too small to make any significant contribution to the scattering, particularly given the low Zr content, and hence would make no sense to include within the RMC model.

The RMC models consisted of 5000 atoms in a cubic box of side 41.5 Å, with periodic boundary conditions. This should allow for correlations up to approximately 20 Å, making calculation of scattering intensities possible to the lowest values of Q measured (0.3 Å^{-1}). The maximum moment correlation length calculated from small-angle scattering results has been found to be 27 Å at T_c [16]. In order to investigate magnetic correlations of this length it would be necessary to use models with an order of magnitude more atoms. This would be very time consuming and expensive, so we decided to use this smaller model, although there are some minor problems with truncation effects. Magnetic moment configurations were created by placing a moment vector at each Fe location in the atomic configuration. Both fully ordered and completely disordered moment configurations have been used as starting points to confirm that the final magnetic structure was independent of the initial magnetic structure.

As there is not yet a version of the magnetic modelling programme, RMCSPIN, which can also deal simultaneously with neutron, x-ray and EXAFS data, we have had to use an iterative procedure. The first step was to fit the neutron data. Using standard RMC criteria [1, 16] for accepting or rejecting atomic moves and magnetic moment rotations, the configurations are updated until suitable agreement between the experimental and calculated structure factors is achieved. Upon convergence the result is a three dimensional atomic structure and a three dimensional magnetic moment structure, which together are consistent with the neutron diffraction data within experimental error. Figure 2 shows the RMC fit to the neutron data at 150 K. As can be seen the weak peak at 1.2 Å^{-1} is found in the magnetic part of the structure factor.

Having made an initial separation of the atomic and the magnetic parts of the structure factor, we have used the atomic structure from the fit to neutron data as a starting point for an RMC fit to the x-ray data (figure 3). We then returned to the RMCSPIN program and the SLAD neutron data. Keeping the atomic structure invariant and only allowing for magnetic moment rotations, all five temperatures were fitted. No constraints were applied to the total magnetization, which was found to vary from 1.2 μ_B per Fe atom for 10 K to 0.7 μ_B for 300 K. This is in quite good agreement with other results (experimentally determined to be 1.54 μ_B at 4.2 K [17] and theoretically to be 1.4 μ_B [13]), considering that RMC always tends to produce the most disordered structure that fits the data. The RMC fits to the data are not perfect, and it seems that the oscillations in the fitted magnetic structure factor are too damped compared to those in the data. We believe that this is due to the limited size of the configuration; we have not been able to obtain a better fit to the data with any other parameters. It should therefore be noted that any correlations found in the RMC models are likely to be stronger in reality.

Figure 4 shows the moment–moment correlation function. This does not decay to zero at large r, indicating long range ferromagnetic order. There is a small rise at low r, indicating slightly enhanced local ordering for $r < 10$ Å. The radial and the tangential correlations, $\langle \mu_\parallel \cdot \mu_\parallel \rangle_r$ and $\langle \mu_\perp \cdot \mu_\perp \rangle_r$, differ only by a scale factor (figure 5). This behaviour is very different from what was found for $Dy_{0.7}Ni_{0.3}$ and $Dy_{0.7}Fe_{0.3}$ [1–4]. The Dy compounds were

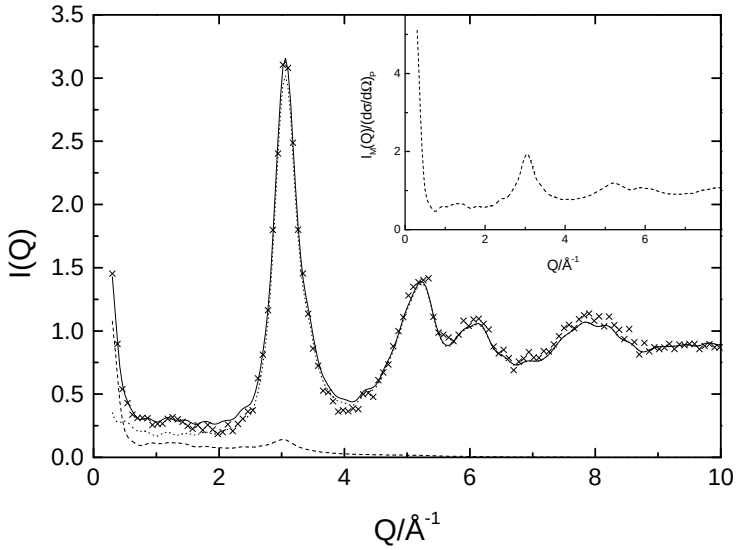

Figure 2. Neutron diffraction data (crosses) at 150 K together with the RMC fit (solid curve) which is the sum of the atomic (dotted line) and magnetic (dashed line) contributions. The inset shows the magnetic structure factor divided by the paramagnetic form factor.

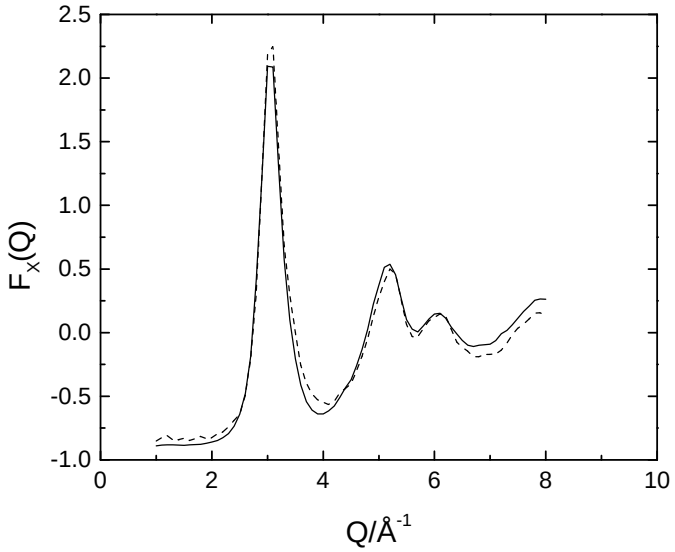

Figure 3. The x-ray diffraction data (solid curve) and the RMC fit (dashed line).

all very anisotropic with detailed tangential correlations, oscillating between ferromagnetic and antiferromagnetic interactions, and almost vanishing radial components. The $Fe_{0.91}Zr_{0.09}$ result then shows that the anisotropy in the Dy compounds was not an artefact of the RMCSPIN modelling procedure.

To analyse the local magnetic ordering, we have calculated the angular correlation between the individual moments and the net magnetization direction, $P_\mu(\cos\theta)$. This is shown in figure 6. We can see that there is a peak at $\cos\theta = 1$ (moments parallel to the magnetization

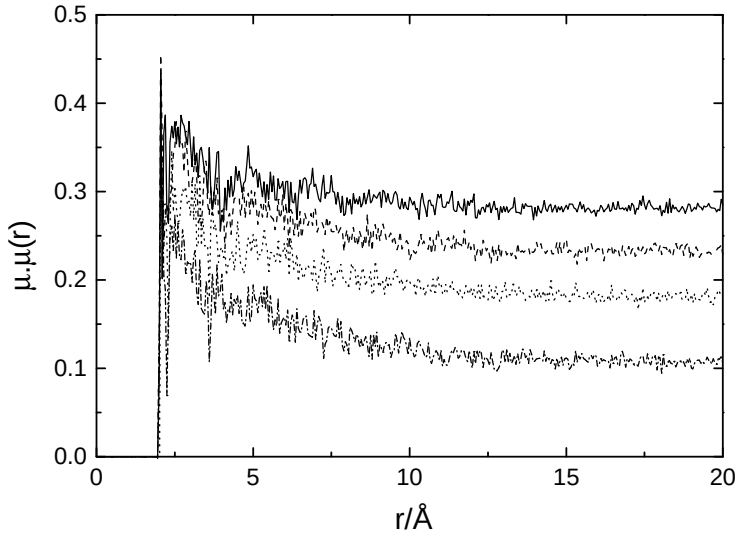

Figure 4. Moment–moment correlation function for $Fe_{0.91}Zr_{0.09}$ at 10 (solid curve), 150 (dash), 200 (dot) and 250 K (dash–dot).

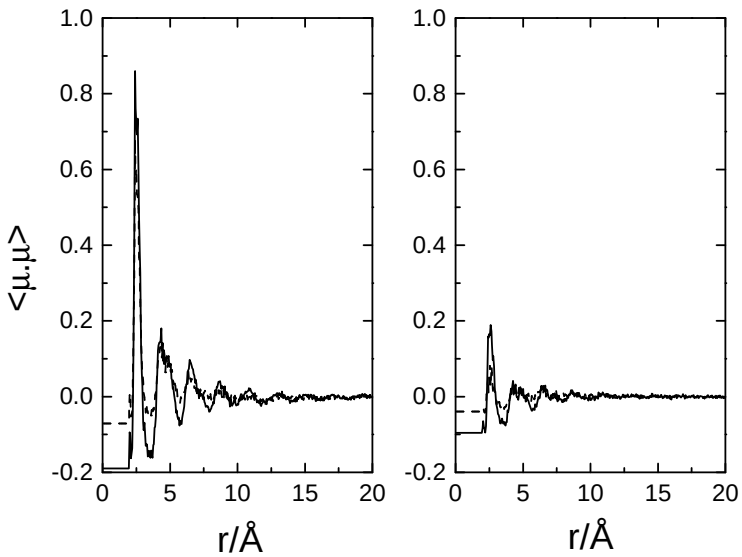

Figure 5. Tangential (left) and radial (right) moment–moment correlation functions for $Fe_{0.91}Zr_{0.09}$ at 10 (solid curve) and 250 K (dash).

direction), indicating generally ferromagnetic coupling with a strength that increases with decreasing temperature, but there are still a number of moments pointing in the opposite direction. In figure 7, the average angle between near neighbour moments, and the average angle between individual moments and the net magnetization direction, are shown as a function of temperature. These extrapolate to $\sim$65 and $\sim 53^\circ$ respectively at 0 K. If we assume that $\mu^2 = 4S(S+1)\ \mu_B^2$ then for a moment of 2.2 μ_B the latter value is close to the expected value of $\cos^{-1}(S/(S(S+1))^{1/2}) = 50^\circ$.

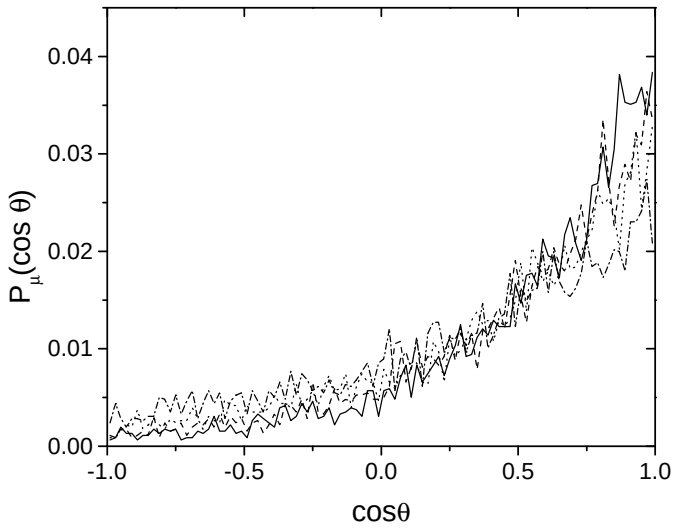

Figure 6. Angular correlation between moments and the net magnetization direction at 10 (solid curve), 150 (dash), 200 (dot) and 250 K (dash–dot).

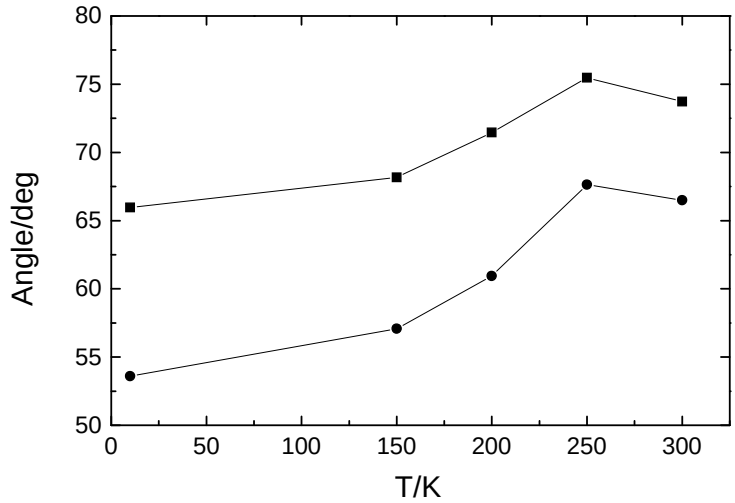

Figure 7. The average angle between near neighbour moments (squares) and the average angle between moments and the net magnetization direction (circles) as a function of temperature.

The average angles at 300 K are lower than those at 250 K, which goes against the trend of increasing angle as T increases (this holds for both LAD and SLAD measurements). We cannot be sure that this is not an artefact caused because the 300 K data were measured separately from the lower temperature data. However it is interesting to note that the most rapid change in average angle occurs at about 225 K, close to the transition temperature $T_c = 218$ K as identified by e.g. susceptibility measurements [9]. This behaviour is similar to that observed in amorphous $Dy_{0.7}Fe_{0.3}$ [4].

The small peak at $Q = 1.2$ Å^{-1} might possibly indicate local antiferromagnetic correlations as it is situated at roughly half the Q value of the main peak. To test this idea

we have separated the moments into two categories, parallel (having $\cos\theta > 0$ in figure 6) or antiparallel ($\cos\theta < 0$) to the average magnetization direction. Figure 8 shows a section from the moment configuration. There are clearly some regions where there are no antiparallel Fe moments, and it can also be seen that near neighbour moments, both parallel and antiparallel, tend to be aligned. In figure 9 we show the partial radial distribution functions, $g_{FeFe}(r)$, for the Fe atoms with different types of moment. The subscripts p and a refer to parallel and antiparallel moments respectively. There is a clear increase in peak height for $g_{aa}(r)$, which means that there is a tendency for the antiparallel moments to be located closer to other antiparallel moments than if they were randomly distributed. This was also verified by calculation of partial atomic structure factors for the different Fe types; $A_{aa}(Q)$ peaks at low Q, which is an indication of clustering of antiparallel atoms. The partial magnetic structure factors for the different types of moment at 10 K are shown in figure 10. Although there are some oscillations, due to truncation, it can easily be seen that the peak at 3 Å^{-1} is a result of ferromagnetic interaction between moments parallel to the magnetization direction; the main contributor is $I_{M_{pp}}(Q)$. The 1.2 Å^{-1} peak is a combination of a peak in $I_{M_{aa}}(Q)$ and a dip in $I_{M_{pa}}(Q)$. This means that it originates predominantly from some interaction involving the antiparallel moments.

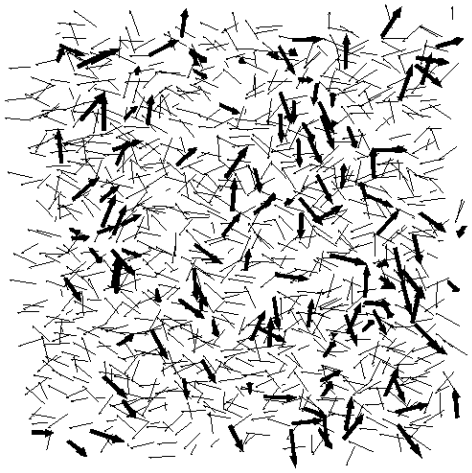

Figure 8. A 10 Å thick section from the moment configuration at 10 K. Antiparallel moments are shown in bold.

5. Discussion

From figure 6 it is obvious that the local ordering in $Fe_{0.91}Zr_{0.09}$ is ferromagnetic at all the temperatures measured. The local magnetic order appears to increase most rapidly at T_c (e.g. figure 7) but this is only a weak effect. However, as $I(Q)$ varies most at lowest Q we do not expect a local ordering transition, but rather a 'domain ordering' transition on length scales above 20 Å, i.e. outside the range of the models produced here. In addition it should be noted that our models are static 'snap-shots' of a structure that is in fact dynamic and hence any 'spin freezing' may only be reflected very weakly in them.

Polarized neutron studies of $Fe_{1-x}B_x$ and similar glasses [18, 19] have proposed a model in which the magnetic structure consists of spins which are 'canted' with respect to the

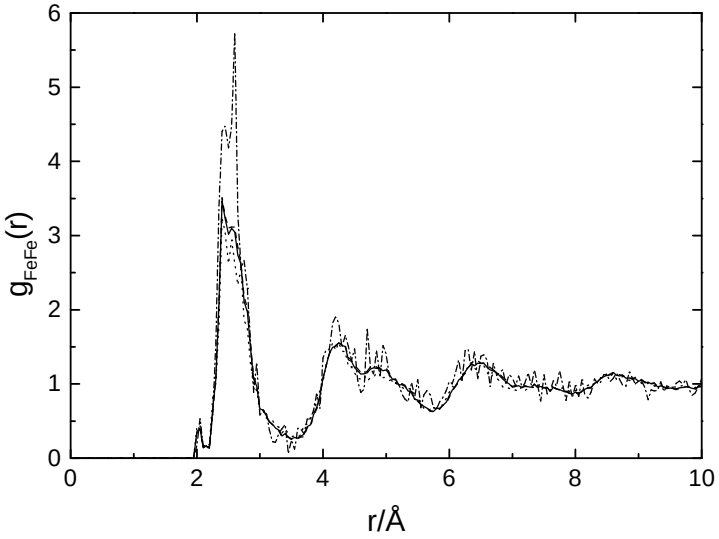

Figure 9. Partial radial distribution functions, $g_{FeFe}(r)$, for Fe atoms with different types of moment (as defined in the text) at 10 K. All atoms (solid curve), parallel–parallel (dash), parallel–antiparallel (dot) and antiparallel–antiparallel (dash–dot).

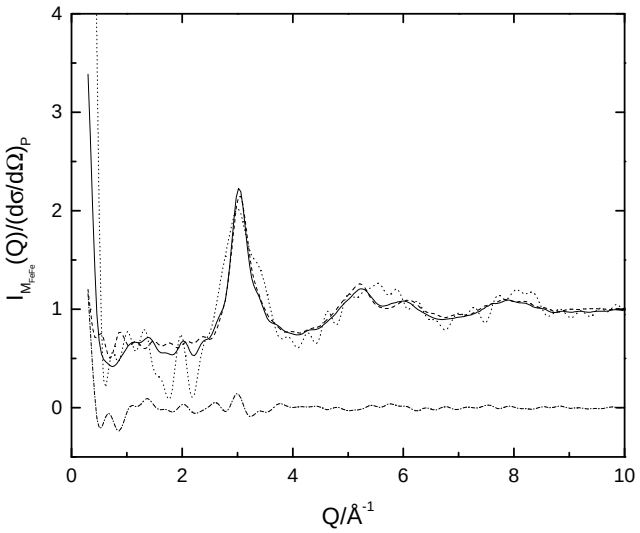

Figure 10. Partial magnetic structure factors for different types of Fe moment at 10 K, divided by the paramagnetic form factor. All moments (solid curve), parallel–parallel (dash), antiparallel–antiparallel (dot) and parallel-pantiparallel (dash–dot). The p–p and a–a structure factors are scaled by 1.155 and 8.4 respectively to give them the same high Q limit as the structure factor for all moments.

magnetization axis, thus explaining that the net moment is lower than the sum of the individual moments. A random distribution of azimuthal angles is assumed. This would mean that the angle distribution in figure 6 consisted of a sharp peak at the average canting angle, while the angular correlation between near neighbour moments would be a broad peak between 0° and

twice the average canting angle. A canting angle of 30° was found for $Fe_{0.83}B_{0.17}$. A recent theoretical study shows canting angles between 0 and 85° for $Fe_{0.8}B_{0.2}$ depending on exchange interaction and density [20]. Our results are consistent with the same order of average angle with the average magnetization direction, ∼60°, but as can be seen from figure 6 this angle in itself has no physical significance. The peak is at 0°. It may therefore be considered that, at least in terms of the models shown here, the canting angle would be a measure of the deviation of the moments from perfect ferromagnetic alignment, rather than a measure of a preferred deviation, i.e. the term 'canting' would be misleading. However it should be noted that there is a characteristic difference in the measured structure factor of $Fe_{1-x}B_x$ glasses, in that they show no low Q rise within the range measured here and no low Q peak (e.g. similar to that at 1.2 $Å^{-1}$ for $Fe_{0.91}Zr_{0.09}$). The canting explanation may therefore be relevant in those cases but not in this.

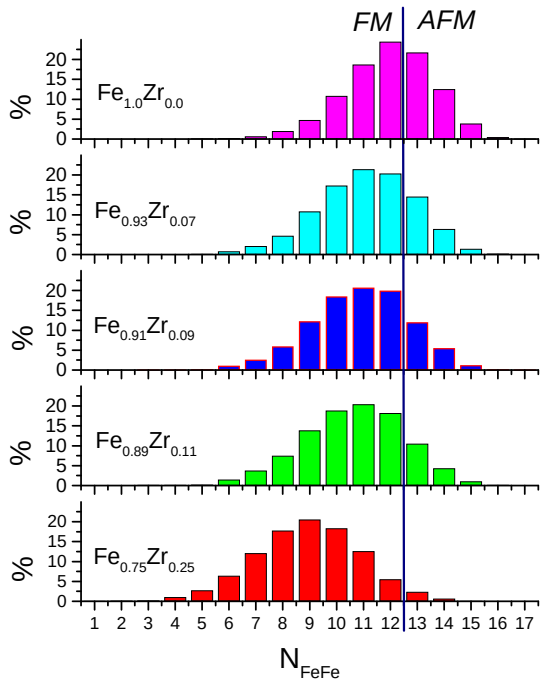

Figure 11. Coordination number distributions, N_{FeFe}, for nearest neighbour Fe atoms within 3.5 Å. The vertical line indicates the boundary between atoms whose interactions are FM or AFM, as defined in the text.

As already indicated in the introduction, it is difficult to compare the models here with other published models for $Fe_{1-x}Zr_x$ glasses, since ours are quantitative models on an atomic length scale whereas the others tend to be 'descriptive' models with unspecified length scales. However we can make some useful comments. Kaul [8] has put forward the idea of ferromagnetic clusters in a ferromagnetic matrix. Generally the idea is that the clusters are rather larger (200 Å) than our models and hence cannot really be compared. However they have suggested that the clusters may be due to the existence of low density regions in the glass, possibly produced during the fabrication process. If this was the case then one would expect some variation in properties between different samples produced by different groups, but in fact the results are remarkably consistent.

In another class of models (e.g. [7]) it is supposed that there are local density fluctuations due to chemical segregation of Zr. Our diffraction data are consistent with a random distribution of Zr, but the scattering contrast between Fe and Zr is not sufficient to rule out some degree of clustering. However the fact that $Fe_{1-x}Zr_x$ glasses can be produced over a very wide range of compositions, and the extremely close values of the atomic radii of Fe and Zr, make it very unlikely that there is any tendency to segregation.

Our results seem to be most consistent with the model of Ryan *et al* [6, 17]. In this (idealized) model the moments are distributed randomly within a cone of half-angle $\psi \sim 30^\circ$ (for $Fe_{0.91}Zr_{0.09}$) relative to the average magnetization direction. This is not inconsistent with our results, particularly as they note that 'a small number of spins rotated by more than 90° from the z-axis... contribute little to R (Mossbauer intensity)' and 'small numbers of antiparallel spins have been observed in Monte Carlo simulations of frustrated Heisenberg systems' [6]. We are unable to say anything about the proposal of spin-glass freezing in the x–y direction at lower T, since as already noted our models are only static. We simply note that we find no evidence of any particular ordering (and hence no change) perpendicular to the average magnetization direction.

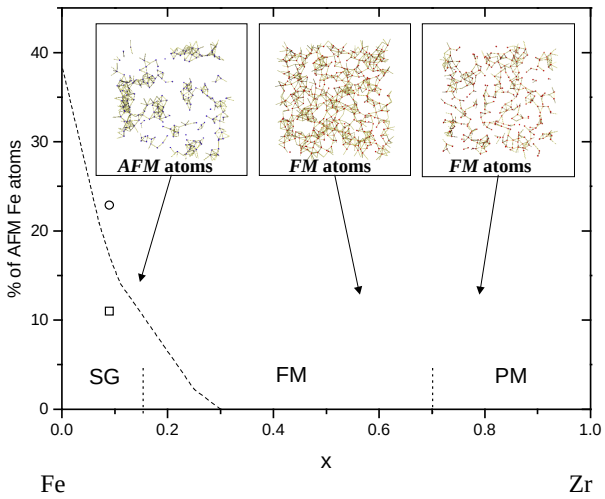

Figure 12. Percentage of AFM Fe atoms (i.e. those with 13 or more Fe neighbours) as a function of x in models of $Fe_{1-x}Zr_x$ glasses (broken curve). The experimentally determined paramagnetic (PM), ferromagnetic (FM) and spin glass (SG) regions are identified. The percentage of antiparallel moments in the RMC models for the magnetic structure of $Fe_{0.91}Zr_{0.09}$ at 10 (square) and 250 K (circle) are also indicated. The insets show the distributions of AFM atoms for $x = 0.09$ and FM atoms for $x = 0.6$ and 0.75.

All of the models originate from the idea of magnetic frustration due to competing interactions, ferromagnetic–antiferromagnetic in two cases and ferromagnetic–ferromagnetic in one. We have identified regions in the magnetic structure where there are spin 'defects' of some type, though they are too small to say whether they can be considered ferromagnetic or antiferromagnetic. All of the models identify the origin of the differing types of interaction as being fluctuations in the local Fe density, as do the theoretical calculations of Lorenz and Hafner [14]. We can show how such fluctuations arise naturally as a result of structural disorder in glasses. While the average Fe–Fe near neighbour coordination in $Fe_{0.91}Zr_{0.09}$ is 10.88 (within 3.5 Å, the distance of the first minimum in $g_{FeFe}(r)$), the coordination of individual atoms can

vary between 3 and 17. (The average coordination of Zr around Fe is 1.05, and the distribution varies between 0 and 6.) We have made the assumption that Fe and Zr substitute isomorphously in $Fe_{1-x}Zr_x$ glasses (which is supported by the close values of the atomic radii and the wide range of compositions over which they can be made) and hence have created a series of structural models for different compositions purely by random substitution of Fe and Zr in our model for $Fe_{0.91}Zr_{0.09}$ glass. We have then assumed (without prior justification) that Fe atoms with 12 or less Fe neighbours interact *ferromagnetically* (FM) and those with 13 or more neighbours interact *antiferromagnetically* (AFM), the italics being used to indicate that these are purely definitions based on coordination number. The coordination number distributions are shown in figure 11. Figure 12 then shows the percentage of AFM atoms as a function of composition on the basis of these definitions. For $x > 0.75$ (25% Fe) all Fe atoms are FM but do not form a connected network of near FM neighbours (see figure 12), so there is only short range magnetic order. The system is therefore paramagnetic. For $0.75 > x > 0.25$ there are no AFM atoms, but the FM atoms form a connected network (figure 12) so the system has long range ferromagnetic order. Below $x = 0.25$ the number of AFM atoms starts to increase, as shown in the figure; initially there are only isolated atoms, but in the region $0.15 > x > 0.05$ there will be sufficient to cause some degree of frustration and hence spin-glass-like behaviour. At $x \sim 0.05$ the AFM atoms themselves form a connected network and so here the frustration would be maximized. These predictions are in remarkably good agreement with the magnetic phase diagram for these glasses. We find that the predicted number of AFM atoms from our structural model for $Fe_{0.91}Zr_{0.09}$ is in reasonable agreement with the number obtained from the antiparallel moments in the RMC magnetic structure (there are two values for the latter since this changes as a function of temperature). The average Fe–Fe coordination number for antiparallel moments in the RMC model for $Fe_{0.91}Zr_{0.09}$ is $\sim$13, while that for parallel moments is $\sim$10, i.e. the spin 'defects' are indeed associated with regions of higher local Fe density. This also agrees with our initial empirical choice of a coordination number of 12 for the division between different types of interaction.

One more comment should be made. For x close to 0.25 the AFM atoms are isolated but as x decreases they will, even if randomly distributed, start to form some form of larger clusters (figure 12). At $x \sim 0.05$ they form a connected network (percolation transition). The correlation length for antiferromagnetic correlations will therefore vary rapidly as a function of x in this region—indeed the structure is likely to be fractal and hence there will be a wide range of correlation lengths. It is therefore perfectly possible that different techniques, which probe the magnetic correlations on different length scales, will indeed find evidence for 'clusters' of different sizes. As we have indicated, these 'clusters' arise naturally as a result of the local atomic density fluctuations within such an amorphous material.

6. Conclusions

RMC modelling of the atomic and magnetic structures of $Fe_{0.91}Zr_{0.09}$ glass has led to the identification of magnetic 'defects', i.e. a small number of moments that point in the opposite direction to the net magnetization. We have proposed these may be caused by local fluctuations in the density of Fe atoms, which are a normal feature of metallic glasses. This proposal is supported by the observation that the magnetic 'defects' have on average a relatively high coordination. Using the RMC structural model for $Fe_{0.91}Zr_{0.09}$ we have then produced models for different glass compositions which enable us to explain the composition dependence of the magnetic phase diagram. This should be tested by further experiments on samples of $Fe_{1-x}Zr_x$ with different values of x.

References

[1] Keen D A and McGreevy R L 1991 *J. Phys.: Condens. Matter* **3** 7383
[2] Keen D A, McGreevy R L, Bewley R I and Cywinski R 1995 *Nucl. Instrum. Methods Phys. Res.* A **354** 48
[3] Keen D A, Bewley R I, Cywinski R and McGreevy R L 1996 *Phys. Rev.* B **54** 1036
[4] Karlsson L, Wannberg A, McGreevy R L and Keen D A 1998 *Phys. Rev.* B submitted
[5] Hannon A C, Wright A C and Sinclair R N 1991 *Mater. Sci. Eng.* A **134** 883
[6] Hong Ren and Ryan D H 1995 *Phys. Rev.* B **51** 15 885
[7] Saito N, Hiroyoshi H, Fukamichi K and Nakagawa Y 1986 *J. Phys. F: Met. Phys.* **16** 911
[8] Kaul S N, Siruguri V and Chandra G 1992 *Phys. Rev.* B **45** 12 343
[9] Gómez-Plaza D, Fernández Barquin L, García Soldevilla J C, Antras R and Gómez-Sal J C 1997 *Solid State Commun.* **102** 353
[10] Zetterström P and McGreevy R L 1998 private communication
[11] Blech I A and Averbach B L 1964 *Physica* **1** 31
[12] Lisher E J and Forsyth J B 1971 *Acta Crystallogr.* A **27** 545
[13] Turek I, Becker Ch and Hafner J 1992 *J. Phys.: Condens. Matter* **4** 7257
[14] Lorenz R and Hafner J 1995 *J. Magn. Magn. Mater.* **139** 209
[15] Rhyne J J and Fish G E 1985 *J. Appl. Phys.* **57** 3407
[16] McGreevy R L and Pusztai L 1988 *Mol. Simul.* **1** 359
[17] Ryan D H, Coey J M D, Batalla E, Altounian Z and Ström-Olsen J O 1987 *Phys. Rev.* B **35** 8630
[18] Cowley R A, Patterson C, Cowlam N, Ivison P K, Martinez J and Cussen L D 1991 *J. Phys.: Condens. Matter* **3** 9521
[19] Wildes A R, Cowley R A, Al-Heniti S, Cowlam N, Kulda J and Lelièvre-Berna E 1998 *J. Phys.: Condens. Matter* **10** 2617
[20] Liebs M and Fähnle M 1996 *J. Phys.: Condens. Matter* **8** 3207